Chemical Science

EDGE ARTICLE

View Article Online
View Journal | View Issue

Cite this: *Chem. Sci.*, 2016, **7**, 3900

Unraveling innate substrate control in site-selective palladium-catalyzed C–H heterocycle functionalization†

Hwanho Choi,[a] Minsik Min,[bc] Qian Peng,*[a] Dahye Kang,[bc] Robert S. Paton*[a] and Sungwoo Hong*[bc]

Understanding the regioselectivity of C–H activation in the absence of directing groups is an important step towards the design of site-selective C–H functionalizations. The Pd(II)-catalyzed direct arylation of chromones and enaminones provides an intriguing example where a simple substitution leads to a divergence in substrate-controlled site-selectivity. We describe computational and experimental studies which reveal this results from a switch in mechanism and therefore the selectivity-determining step. We present computational results and experimentally measured kinetic isotope effects and labelling studies consistent with this proposal. The C–H activation of these substrates proceeds *via* a CMD mechanism, which favors more electron rich positions and therefore displays a pronounced kinetic selectivity for the C3-position. However, C2-selective carbopalladation is also a competitive pathway for chromones so that the overall regiochemical outcome depends on which substrate undergoes activation first. Our studies provide insight into the site-selectivity based on the favorability of two competing CMD and carbopalladation processes of the substrates undergoing coupling. This model can be utilized to predict the regioselectivity of coumarins which are proficient substrates for carbopalladation. Furthermore, our model is able to account for the opposite selectivities observed for enaminone and chromone, and explains how a less reactive coupling partner leads to a switch in selectivity.

Received 28th November 2015
Accepted 2nd March 2016

DOI: 10.1039/c5sc04590h

www.rsc.org/chemicalscience

Introduction

Palladium-catalyzed C–H bond activation is an efficient, atom-economical tool in the synthesis of functionalized organic molecules.[1–4] However, the ability to activate a specific 'inert' C–H bond in the presence of several others dictates that control must be exerted over the position of activation. This challenge lies at the forefront of developments in synthetic methodology. One such strategy to achieve high site-selectivity is the use of directing groups covalently tethered to the substrate, which coordinate to the transition-metal center and direct C–H activation to a proximal site. Significant developments in terms of *ortho*,[1,2] *meta*[3] and *para*-directing[4] groups have been accomplished for aromatic C–H activation. However, an alternative approach – free from directing groups – is to exploit the inherent electronic and steric preferences of both catalyst and substrate to control the regiochemical outcome of C–H functionalizations according to innate reactivities. While controlling the cleavage of a specific C–H bond among several others remains a significant challenge, access to fundamental mechanistic insights into C–H bond activation has been possible from combined computational and experimental investigations.[5,6] By adopting such an approach, we now explain contrasting regioselectivities of electron-rich heterocyclic C–H functionalizations, with the intention of providing a rational basis for the design of site-selective catalytic C–H activation.

A breakthrough in the regioselective Pd-catalyzed C–H functionalization of indoles was made by Fagnou and coworkers.[7] Davies and Macgregor first provided a theoretical basis for understanding C–H activation with $Pd(OAc)_2$ in terms of ambiphilic metal ligand activation (AMLA),[8] where the Pd-coordinated acetate acts as proton-abstracting base. Analysis of a wide range of aromatic and heteroaromatic substrates by Fagnou and Gorelsky led to the generalization of this mechanism, termed concerted metalation–deprotonation (CMD) mechanism.[9] Since the pioneering work by Fagnou, significant progress has been made to synthesize a variety of bi(hetero)aryl scaffolds *via* oxidative C–H/C–H cross-coupling approach. Computational studies have been performed to gain considerable insight into Pd-catalyzed C–H functionalization in the presence of directing groups, for both $C(sp^3)$–H and $C(sp^2)$–H

[a]*Chemistry Research Laboratory, Department of Chemistry, University of Oxford, 12 Mansfield Road, Oxford OX1 3TA, UK. E-mail: qian.peng@chem.ox.ac.uk; robert.paton@chem.ox.ac.uk*

[b]*Center for Catalytic Hydrocarbon Functionalizations, Institute for Basic Science (IBS), Daejeon, 34141 Korea. E-mail: hongorg@kaist.ac.kr*

[c]*Department of Chemistry, Korea Advanced Institute of Science and Technology (KAIST), Daejeon, 34141 Korea*

† Electronic supplementary information (ESI) available. See DOI: 10.1039/c5sc04590h

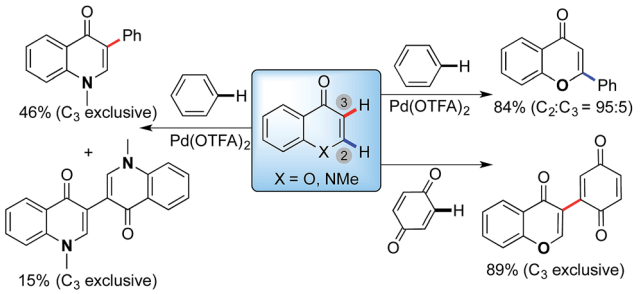

Scheme 1 Divergent site-selectivity in the Pd-catalyzed direct arylation of enolone (X = O) and enaminone (X = NMe) substrates with arenes. Standard conditions: $Pd(OTFA)_2$ (20 mol%) and AgOAc (3.0 eq.) in pivalic acid at 100 °C.

activation.[10–12] However, mechanistic aspects of C–H bond activation involving non-aromatic substrates remain elusive and predictions of selectivity in the absence of directing groups are difficult. This is exemplified by enolone and enaminone heterocycles: these structures differ only in the identity of a single heteroatom, however, the site of functionalization is completely different under identical conditions, as depicted in Scheme 1.[13] The mechanistic basis for this difference has thus far been unexplained.

We recently described the Pd(II)-catalyzed regioselective arylation of chromones and enaminones with simple arenes *via* a two fold C–H bond functionalization (Scheme 1).[13a,b] The pivalate and other bidentate anions have been proposed to act as a catalytic proton shuttle,[7] lowering the activation energy of Pd-catalyzed C–H bond cleavage. In our studies, contrasting regioselectivities are observed in the reactions of chromone (X = O) and enaminone (X = NMe) substrates (Scheme 1). The C-2 arylation of chromones proceeded with high regioselectivity (C2 : C3 = 95 : 5).[13c] Substrates conjugated with a variety of functional groups from electron-donating to electron-withdrawing groups were tested, and the C2-arylated products were obtained with high regioselectivity (~20 : 1) in all cases. On the other hand, the C-3 arylation product was exclusively obtained with the enaminone substrate under the same reaction conditions. Furthermore, coupling of chromone with *para*-benzoquinone also results in a switch to complete selectivity for the C3-position.[13d] Consequently, we reasoned that the regioselectivity of this oxidative cross-coupling is dramatically affected by the intrinsic properties of the substrates (enaminone *vs.* enolone). Intrigued by the dramatic change in regioselectivity with subtle alterations (N *vs.* O) in the substrates, we further investigated to elucidate the origin of the high level of selectivity with density functional theory (DFT) and experimental isotopic labeling studies.

Results and discussion

Isotopic labeling studies

The rate of C–H activation of chromone was investigated experimentally by following the incorporation of deuterium in D_2O (Scheme 2). Partial deuteration (40%) takes place in 6

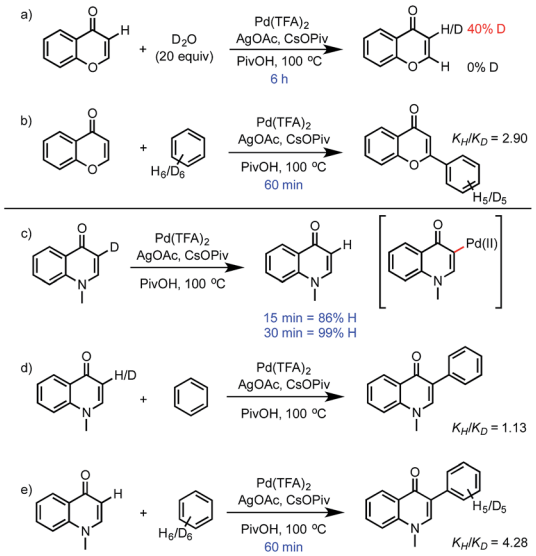

Scheme 2 Isotopic labeling studies of chromone and enaminone.

hours, while for enaminone the loss of deuterium is complete within 30 min at the same C3-position. There is no evidence of exchange at the C2-position of either substrate, even though arylation of chromone occurs at C2. This led us to consider the different possible mechanisms to account for these observations.

Computational studies. We considered sequential arene C–H activation occurring at a single Pd(II)-center followed by reductive elimination to form the C–C bond and Pd(0) (Scheme 3). The activation of benzene may precede enolone/enaminone activation, as in mechanism (a), or with the alternate sequence of C–H activation steps as in mechanism (b). Additionally, the possibility of carbopalladation occurring as the second step was also computed.

Several potential mechanisms may be conceived for $C(sp^2)$–H activation by a Pd(II)-center (Fig. 1a). We investigated chromone and enaminone substrates undergoing C–H activation by the $Pd^{II}(OTFA)_2$ catalyst *via* electrophilic aromatic substitution (S_EAr),[12] a termolecular electrophilic substitution (S_E3)[14] and concerted metalation–deprotonation (CMD)[15] pathways. In

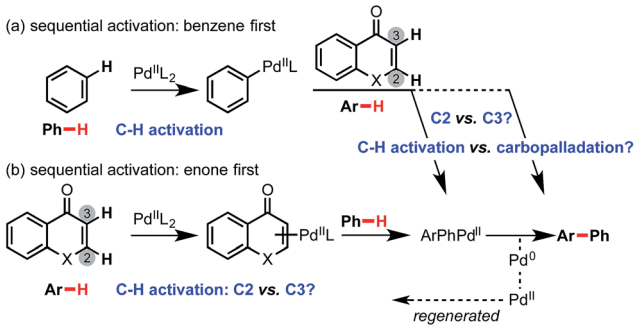

Scheme 3 Mechanistic possibilities investigated for Pd-catalyzed oxidative cross-coupling with enolone (X = O) or enaminone (X = NMe) with benzene.

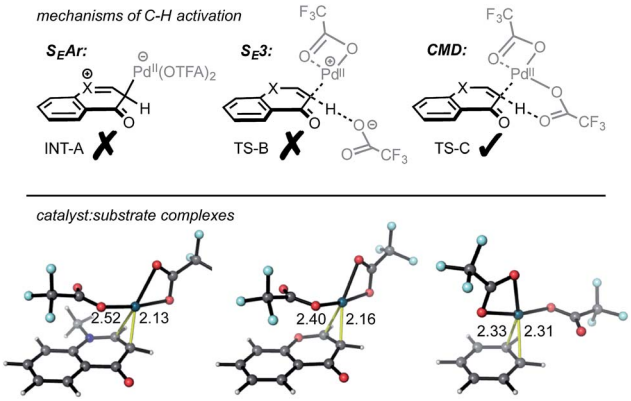

Fig. 1 Top: C–H activation mechanisms considered: electrophilic aromatic substitution (S_EAr), termolecular electrophilic substitution (S_E3) and concerted metalation–deprotonation (CMD). Bottom: catalyst–substrate complexes with distances in Å.

accord with previous computational results,[11b] we were unable to locate any stable structures corresponding to the formal Wheland intermediate (**INT-A**). Attempts to optimize transition structures (**TS-B**) corresponding to proton abstraction following electrophilic activation by a cationic $PdOTFA^+$ species (S_E3 mechanism) were similarly unsuccessful, resulting in the location of CMD transition structures. Mechanisms involving C–H oxidative insertion and σ-bond metathesis have been shown to give dramatically higher activation barriers than CMD and were thus not considered further.

The interaction of $Pd(OTFA)_2$ with the C2/C3 π-bond of both substrate is characterized by a single η^2-bound conformation (Fig. 1b): the catalyst is positioned closer to the C3 position due to the greater π-electron density at this position which is more pronounced for enaminone than chromone. In contrast, coordination to benzene is nearly symmetrical. For the CMD pathway, **TS-C** (at both C2 and C3 positions), was characterized and provides a viable mechanism of C–H activation for all three arenes. The absence of stationary points corresponding to **INT-A** and **TS-B** cannot absolutely preclude their existence (absence of evidence is not evidence of absence!), nonetheless, CMD activation barriers and thermochemistry are consistent with experimentally observed hydrogen–deuterium exchange at the C3 position and not at the C2 position (Scheme 2).

Arylation of chromone. In the Pd-catalyzed coupling of chromone with benzene, the first C–H activation event may occur at either of the C2 or C3 positions of chromone, or may involve benzene instead (Fig. 2, first C–H activation). The preference for C–H activation of chromone at the C3 position (*via* **TS-3**) is dramatic, such that the barrier for C2 activation is prohibitively large (9.2 kcal mol^{-1} relative to **TS-3**). This difference is striking: the innate kinetic preference for C–H activation at the C3-position of chromone contrasts with the high level of selectivity observed for C2-arylation. Even bearing in mind potential computational inaccuracy, the large computed C2/C3 reactivity difference show that this C–H activation step is not involved in determining overall regioselectivity. The much greater reactivity at the C3 position results from the greater π-electron density at this position: π-Lewis acidity and C–H strength both influence CMD reactivity,[16] and the variation in the former is evidently greater than the latter for chromone. Additionally, we have confirmed this prediction experimentally: under arylation conditions, we observe H/D exchange (Scheme 2a) at the C3-position, which is consistent with reversible C–H abstraction and protonation of the palladated intermediate by the acidic solvent on a timescale commensurate with the computed activation barrier of 21.6 kcal mol^{-1} (see ESI†). We also confirmed that the formation of C2-deuterochromone was not observed within six hours, which is consistent with the prediction of exclusive reactivity at C3, and a high barrier for the C2-position. This supports our assertion that C2-selectivity does not arise from preferential C–H activation at this position.

In fact, the C–H activation of benzene *via* CMD **TS-1**, is computed to occur more quickly than for either position of chromone – the free energy barrier is 1.2 kcal mol^{-1} lower than for the C3-activation. This activation of benzene benefits from the statistical effect of a 40-fold excess of benzene use experimentally, and also from the presence of six equivalent C–H bonds. In addition to a lower barrier, the thermochemistry of benzene activation is also more favorable, forming arylpalladium species (intermediate **3**) which is more stable than either position of chromone. Given the preferential reactivity of benzene towards C–H activation and the greater stability computed for the arylpalladium intermediate formed, we investigated the subsequent reaction of the phenylpalladium intermediate with chromone. Firstly, we considered the potential for a second CMD processes in which the phenylpalladium species activates the C2 and C3 positions of chromone. Followed by (irreversible) reductive elimination, this process leads to the coupled heterobiaryl product (Fig. 2 second C–H activation and reductive elimination). As with the CMD TSs involving $Pd(OTFA)_2$, a sizable difference in reactivity is computed in favor of CMD activation at the C3 position (*via* **TS-4** and **TS-5**). This preference is a result of the greater π-electron density at the C3-position. This C–H activation step has a higher computed barrier than the initial activation of benzene and lies above the subsequent reductive elimination step. This mechanism cannot account for the high level of C2-arylation selectivity, since this isomer is kinetically disfavored by a much high barrier for the second CMD step. Nor can it account for the observed primary KIE when benzene-d_6 is used (Scheme 2b), and so this mechanism was rejected.

We investigated an alternative to sequential CMD steps: a migratory insertion/carbopalladation of the phenylpalladium intermediate across the isolated π-bond of chromone (Fig. 3). Arylpalladium species are known experimentally to add across the π-bonds of enones, which have been studied computationally.[17] Prior to locating the TS structures for this process, we carried out an exhaustive 2D-scan of the potential energy surface (see ESI†) in which the distances between the phenyl *ipso*-carbon and C2 and C3 positions of chromone defined the search coordinates. This established the existence of two carbopalladation TSs and also confirmed that there is no feasible means of interconversion between the two adducts. Regioisomeric structures **TS-8** and **TS-9** were found to lie much lower in

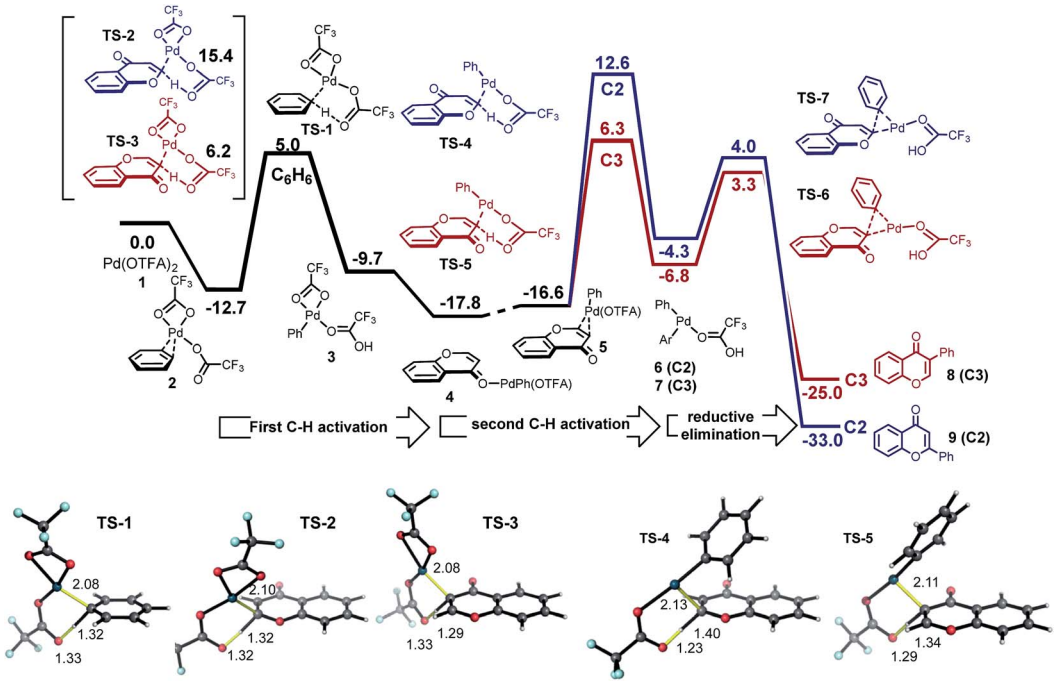

Fig. 2 Coupling of chromone and benzene *via* sequential C–H activation. Palladation of benzene (40-fold excess) with $Pd(OTFA)_2$ is marginally faster than for the C3-position of chromone; palladation of chromone by PhPd(OTFA) and subsequent reductive elimination: the C3-regioselectivity afforded by this mechanism is inconsistent with experiment. Structures are colored as follows: Pd (dark blue), F (light blue), O (red), C (grey), H (white).

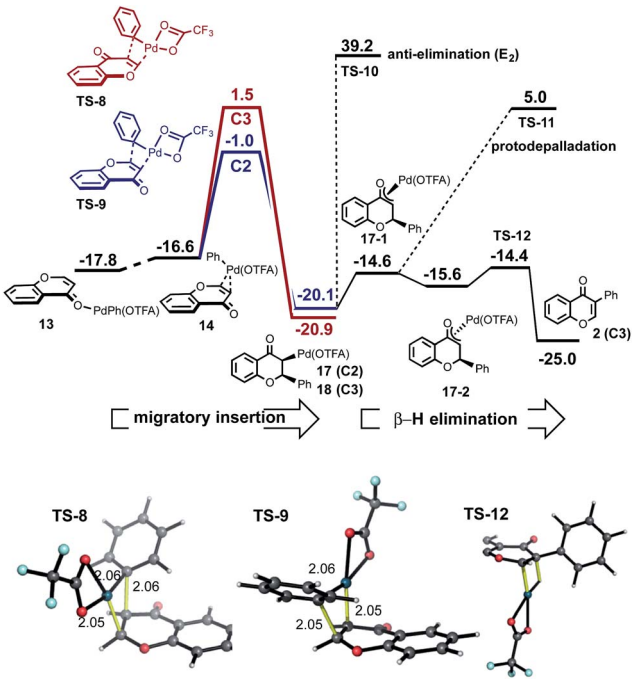

Fig. 3 Migratory insertion/carbopalladation of PhPd(OTFA) across the π-bond of chromone is favored relative to CMD; the correct C2-regioselectivity is computed from this step, which is irreversible.

free energy than those structures previously obtained for the CMD-reductive elimination pathway (Fig. 3, migratory insertion). While caution should be exercised in comparing different mechanisms, the difference of more than 7 kcal mol^{-1} in favor of carbopalladation lends rather strong support for this mechanism.

Additionally, the relative stability of carbopalladation TSs is consistent with the observed level of C2-selectivity for chromone arylation: the experimental value of 95 : 5 compares very favorably with our computed selectivity of 97 : 3 based on a $\Delta\Delta G^{\ddagger}$ of 2.5 kcal mol^{-1} between **TS-8** and **TS-9**. Our calculations support the view that the subsequent steps following carbopalladation are relatively facile, making carbopalladation itself irreversible and therefore the regiodetermining step in chromone arylation (Fig. 3, β-H elimination).

The greater π-electron density at the C3-position of chromone favors the delivery of the electrophilic Pd(OTFA) center to this position in **TS-9**, which leads to the C2-delivery of the phenyl group in the carbopalladation step. Our prediction of a preference for chromone towards carbopalladation rather than concerted metalation–deprotonation can be understood in terms of the inherent reactivity of the α,β-unsaturated C=C bond, which although conjugated is not part of an aromatic ring system. In contrast, (hetero)aromatic systems would be expected to resist the loss of aromaticity which necessarily results from carbopalladation and will favor the CMD pathway where this is less severe. The KIE value, $k_H/k_D = 2.90$ observed for benzene-h_6/d_6 suggests turnover-limiting C–H cleavage of benzene (Scheme 2b), consistent with our calculations in which the initial C–H activation of benzene has a higher barrier than the subsequent carbopalladation step.

Conversion of the intermediate following carbopalladation into the arylated product could occur *via* an (E_2) *anti*-elimination **TS-10** or alternatively, epimerization *via* a Pd-enolate and subsequent *syn* β-hydride elimination **TS-12** (Fig. 3). Alternatively, protonolysis of the intermediate would lead to the product of conjugate addition of the phenyl group to the enone (**TS-11**). Although this is not observed in our experiments, different solvents have been shown to lead to a switch between arylation and conjugate addition products.[18] The computed barrier to *anti*-elimination is highly uncertain, since the identity of the external base is unknown, however with an anionic trifluoroacetate the barrier to this step is prohibitively high. In contrast, *syn* β-hydride elimination is facile, provided the intermediate is able to interconvert to the epimeric form (from π-coordinated **10-1** to **10-2** *via* free rotation in the O-bound enolate) in which the metal is now on the same side of the ring as the β-hydrogen.

The regioselectivity of chromone does not arise from the site-selectivity of C–H activation, since in this respect the C3-position is kinetically favored. Rather, with benzene undergoing C–H activation first, carbopalladation of chromone becomes the selectivity-determining step. The computed regioselectivity of migratory insertion by 2.5 kcal mol^{-1} accounts quantitatively for the experimentally observed preference for C2-arylation. Sequential C–H activation at a single Pd(II)-center (in either order), followed by reductive elimination is uncompetitive, with activation barriers over 7 kcal mol^{-1} higher than the favored carbopalladation route and predicts the incorrect regioselectivity. Based on this new understanding, we realized that C3-selective arylation of chromone should result whenever C–H activation becomes the selectivity-determining step. For example, by coupling with a partner which is much less prone to undergo C–H activation, but is itself a proficient substrate for carbopalladation, such as *p*-benzoquinone (Fig. 4) this should be possible. Indeed, our calculations confirm that *p*-benzoquinone is much less reactive towards C–H activation (CMD **TS-21** lies significantly higher in free energy than reaction at the C3 position of chromone, by 8.7 kcal mol^{-1}). Therefore, for this coupling the C–H activation of chromone occurs first. Conversely (unlike benzene), *p*-benzoquinone is a good substrate towards carbopalladation, and so the intrinsic reactivity towards C–H activation at the C3-position of chromone ensures selectivity for this regioisomer. The very high levels of selectivity ($\Delta\Delta G^{\ddagger}$ of 9.2 kcal mol^{-1}) predicted by this model supports our previous experimental observations of the coupling(s) of chromone with *p*-benzoquinone[13d] and alkenes,[19] which occur exclusively at the C3-position.

Arylation of enaminone. We turned our attention to the arylation of enaminone, where reaction with benzene under identical conditions to those used for chromone led to opposite regioselectivity. The hetero-coupled product was formed exclusively as the C3-isomer, while enaminone C3–C3 homocoupling is also observed as a minor product. Considering potential C–H activation of the substrate by $Pd(OTFA)_2$, we now see that the barrier to CMD at the C3-position is lower (**TS-16**) than that computed for chromone or benzene (Fig. 5). Additionally, the stability of the enaminone C3-palladated intermediate is greater

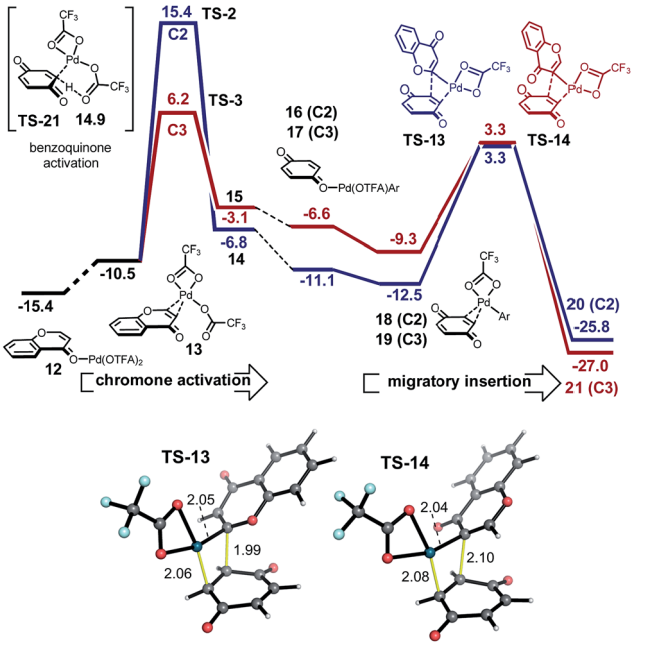

Fig. 4 Coupling of chromone and *p*-benzoquinone *via* a C–H activation–carbopalladation sequence; C3-regiochemistry is predicted and observed experimentally.

for enaminone than for chromone, such that this now becomes feasible as a first step in the mechanism. The steric contribution associated with the N–Me group has a negligible effect upon selectivity of C–H activation: there are no obvious close contacts in **TS-15**, and the energy difference was unaffected when a model N–H enaminone substrate was computed separately.[38]

The ease and reversibility of C–H activation of enaminone at the C3-position suggested by the computed reaction coordinate in Fig. 5 was confirmed experimentally (Scheme 2c). Exposure of C3-deuterated enaminone substrate to the catalytic reaction conditions in the absence of benzene, led to 99% conversion to the C3-protio form within 30 minutes. Reaction times required for benzene heterocoupling take much longer (on the order of 8 hours), which suggests that enaminone C–H activation cannot be turnover-limiting in this process. Attempts to obtain primary kinetic isotope effect (KIE) measurements for C3-deutero-enaminone are complicated by scrambling of the D atoms in the substrate: based on conversion after 60 min a k_H/k_D value of 1.13 was obtained. In contrast, a primary KIE value, $k_H/k_D = 4.28$, was observed based on parallel experiments of benzene and benzene-d_6 with enaminone (Scheme 2e). This suggests turnover-limiting C–H cleavage of benzene,[20] although large intrinsic isotope effects have also been observed in arene oxidative coupling where transmetalation of two bimetallic intermediates is the limiting step.[21,22]

Based on our computational and experimental evidence for facile C3–H activation of enaminone and the comparatively slow C–H activation of benzene, we reason that palladation of enaminone will occur first. C–H activation at the C2 position of enaminone is unlikely to occur due to a significantly higher free energy barrier (33.3 kcal mol^{-1}). Additionally, homocoupling

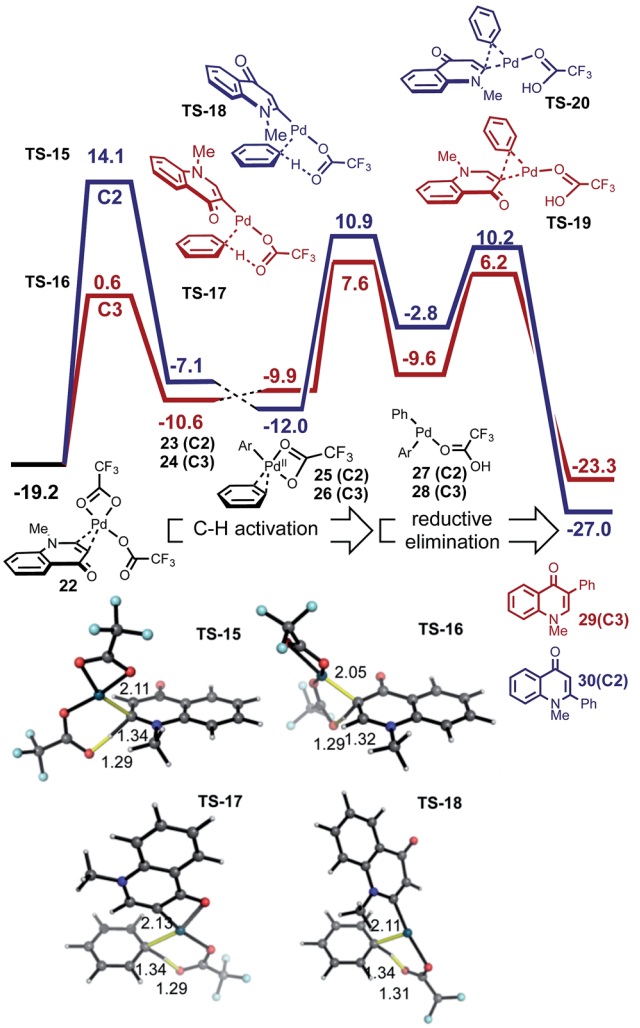

Fig. 5 Sequential C–H activation of enaminone and benzene followed by reductive elimination. The C3-product is kinetically favored.

only shows C–C formation at the C3-position of enaminone.[23] Computed mechanism of CMD activation of benzene and subsequent reductive elimination is shown in Fig. 5. The $\Delta\Delta G^{\ddagger}$ between the regioisomeric pathways amounts to 6.5 kcal mol^{-1} (defined by the difference between turnover-limiting **TS-15** for C2 and **TS-17** for C3 positions) in favor of the C3-product. The passage *via* **TS-16** in step 1, followed by **TS-17** accounts for the C3-selectivity since both CMD TSs along the C2-pathway are less stable. The observed primary KIE with benzene-d_6 is consistent with our computed free energy profile since the turnover-limiting TS is the second CMD activation step in which benzene undergoes C–H activation in **TS-17**. We also computed the analogous mechanism for the homocoupling of enaminone at the C3-position, which is formed in 15% yield. The second CMD-step of homocoupling has a TS of similar stability to **TS-17**, which is 1.3 kcal mol^{-1} lower in free energy. Thus this process is competitive with benzene heterocoupling as found experimentally, although since this mechanism is bimolecular in enaminone it becomes less competitive during the reaction, as substrate is consumed and benzene remains in a large excess. These results show that the turnover limiting step in the arylation of both enolone and enaminone substrates is the C–H activation of benzene, although the catalytic species involved is prediction to be different ($Pd(OTFA)_2$ *vs.* $PdAr(OTFA)_2$). The computed free energy span[24] is 26.8 kcal mol^{-1} for the C3-arylation of enaminone and 20.4 kcal mol^{-1} for the C2-arylation of chromone. This is consistent with the lower reactivity observed for enaminone (as judged by lower conversion obtained experimentally for the latter).

Origins of divergent site-selectivity. We present the energetics for all of the transition structures with $Pd(OTFA)_2$ discussed so far in Scheme 4, organized sequentially by their relative stability. Focusing on the CMD energetics, there is a marked separation according to whether the position undergoing activation is electron rich or electron deficient: the latter group describes the C2-positions of chromone or enaminone along with benzoquinone, and their corresponding barriers are all kinetically unfeasible and *ca.* 10 kcal mol^{-1} higher than for their more electron rich counterparts. Inspection of the electrostatic potential for each of these substrates confirms that the positions of greater electron density undergo C–H activation more easily. For enaminone and chromone the C3-position also provides the greatest atomic orbital contribution to the HOMO (as depicted in the ESI†) and also carries a substantially greater negative charge than at C2 from natural population analysis. The site-selectivity of C–H activation can thus be clearly related to the innate polarization of these substrates. Unlike (hetero) aromatic systems, the greater C=C bond localization in the substrates studied here enables a competitive carbopalladation pathway to occur. The inherent polarization of the C=C bond in chromone and enaminone, and the sites of HOMO/LUMO coefficients act to favor C2-arylation (Scheme 4c) since the metal is delivered to the more electron-rich position in concert with C–C formation.

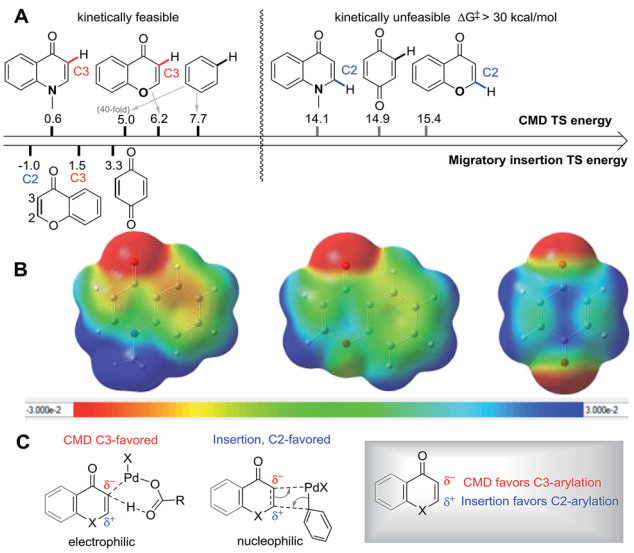

Scheme 4 (A) Energy of key transition states for site-selectivity; (B) electrostatic potential map (ESP) with iso-value = 0.001 C: favorable site-selectivity in the reaction.

The scope of our newly developed mechanistic model is applicable to other substrates and Pd-catalyzed functionalizations, so that we can predict regioselectivity in the arylation and alkenylation for chromone and other heteroamatic substrates, such as coumarins (Scheme 5). Based on the inherent polarization of chromone and coumarin substrates we predict that C–H activation of both substrates will occur preferentially at the enone α-position, and that carbopalladation will deliver the aryl group preferentially to the β-position. Alkenylation is thus expected to result in α-selectivity since heterocyclic CMD-activation dictates selectivity: indeed, experimentally this is the sole regioisomer for each substrate.[19a,b] Conversely, arylation is expected to result in β-selectivity as carbopalladation by the arylpalladium intermediate dictates selectivity, which is seen experimentally for both substrate.[13a,b,19c] Our model is consistent with experimental isotopic labeling studies, which show the C3 (α)-position of coumarin to be most susceptible towards palladation. A significant level of deuterium incorporation (41% D after 12 h) is observed at this position in the presence of D_2O (20 equiv.).[19b] The calculated MOs and ESP map of coumarin (see ESI†) confirm that the polarization is in a similar sense as the other enolones considered, and can thus be used to make tangible predictions of regioselectivity for real catalytic reactions.

Our work illustrates that the site-selectivity of Pd(II)-catalyzed C–H functionalizations will not always correspond to the position which undergoes metalation most quickly. This may seem relatively trivial, although it does establish that universal predictions of site-selectivity that focus on substrate and catalyst alone are impossible. For heterocyclic systems such as we have considered here, where there is a sizable difference in the π-Lewis acidities at different positions, large and opposite selectivities will be attainable depending on whether C–H activation by a CMD mechanism or carbopalladation occurs.

In each case the metal favors delivery to the more electron-rich position. In fact, we observe a strong linear correlation between the activation barriers of the CMD transition states with $Pd(OTFA)_2$ and two geometric parameters in those structures: the C–Pd distance ($R^2 = 0.92$) and the distortion of the C–H bond out of the ring-plane ($R^2 = 0.99$) as shown in Fig. 6. The linear correlation of other structural parameters with reactivity are less quantitatively useful (see ESI†) but provide further support for the electrophilic nature of the C–H activation step. For example, a longer C2=C3 bond is present in the more stable CMD TS structures ($R^2 = 0.83$) due to the resonance contribution from heteroatom lone-pair donation. TS structures which exhibit more agostic character,[25] as judged by a shorter Pd–H distance, are disfavored ($R^2 = 0.78$). While metalation and deprotonation remain concerted in these TS structures, those substrates and positions of activation that are more electron rich benefit from more advanced C–Pd formation in the TS and an ensuing increase in C–H acidity due to the distortion out-of-plane of the *ipso* C–H bond.

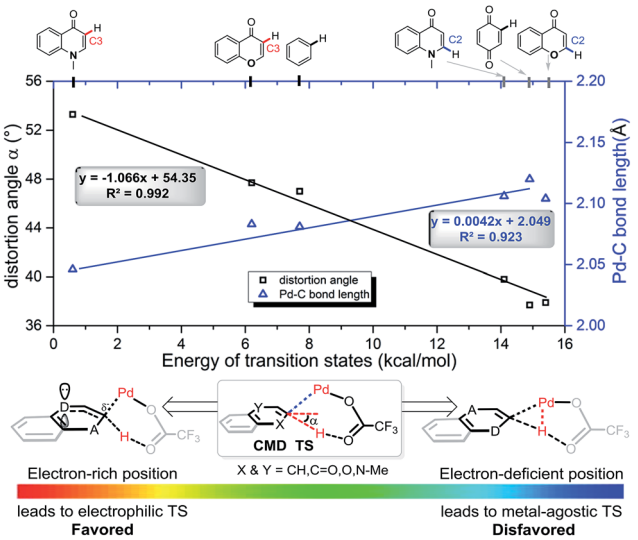

Fig. 6 For all CMD TSs the Pd–C distance and out-of-plane deformation of the C–H bond correlate strongly with the TS energy.

Conclusions

In summary, we have performed a detailed mechanistic study incorporating computational and experimental approaches to account for the divergent site-selectivity in Pd(II)-catalyzed direct arylations of enolones and enaminones. The computed mechanism for the two substrates is consistent with observed regioselectivities and the measured kinetic isotope effects which show benzene activation to be turnover-limiting. C–H activation of these substrates by a CMD mechanism favors more π-electron rich positions and displays a pronounced selectivity for the C3-position of both chromone and enaminone. Exclusive C3-selectivity in enaminone arylation occurs since the C–H activation barrier at C2 is prohibitively high. The carbopalladation of chromone favors the delivery of the aryl group to the C2-position since the metal interacts more strongly at the neighboring C3-site. The divergence in selectivity results from a switch in mechanism between these two competing pathways (CMD *vs.* carbopalladation), and it is possible to reason which will occur based on the inherent reactivities of the substrates towards C–H activation. We have shown that the favorability of CMD and carbopalladation steps can be understood based on

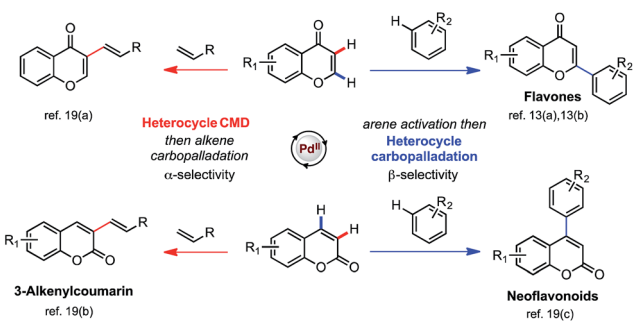

Scheme 5 Experimental regioselectivities of the arylation and alkenylation of chromone and coumarin substrates are in accord with the computational model.

the innate electronics of the reacting species, which forms the basis for rational predictions of site-selectivity. The regioselectivity in C–H functionalization of coumarin substrates can be accurately rationalized by this model.

Methods

Experimental details

To a capped sealed tube were added $Pd(TFA)_2$ (20 mol%), AgOAc (3.0 equiv.) and CsOPiv (3.0 equiv.). Subsequently, 1-methylquinolin-4(1*H*)-one-3 (or deuterated at the C3-position) (0.1 mmol), benzene (or benzene-d_6) (0.5 mL) and pivalic acid (0.5 mL) were added. The reactions were stirred at 100 °C for 60 min. The reaction mixture was cooled to room temperature, and then diluted with CH_2Cl_2 and $NaHCO_3$. After stirring for 10 min, the mixture was washed sequentially with aqueous $NaHCO_3$ and NH_4Cl. The combined organic layers were dried over $MgSO_4$. The filtrate was concentrated *in vacuo* and the yield was analyzed by ^1H NMR.

Computational methods

All stationary points were fully optimized at the density functional theory level in Gaussian 09 (rev. D.01),[26] using the dispersion-corrected ω-B97XD functional[27] without symmetry constraints. The effective core potentials (ECPs) of Hay and Wadt with a double-ζ basis set (LanL2DZ)[28] were used for Pd, and the 6-31G(d) basis set was used for H, C, N, O and F(BS1). The energies were further evaluated using a larger basis set (6-311+G(d,p) basis set for H, C, N, O and F) and a triple-ζ basis set and associated ESP (LanL2TZ(f))[29] for Pd(BS2) by single-point calculations. Single point calculations with the B3LYP functional[30] with a D3-dispersion correction[31] with zero-damping at short range[i] with BS2 were used to corroborate these results – large differences between C2 and C3 C–H activation are also observed with this method and reaffirm the differences in selectivity presented in the manuscript. The effects of solvation were described with an implicit description of acetic acid using the CPCM treatment,[32] where the United Atom Topological Model (UAHF) was used to define the solute cavity. All optimized species were verified as either minima or transition structures by the presence of zero or a single imaginary vibrational frequency. Gibbs free energies were evaluated at the reaction temperature using vibrational frequencies: the rigid rotor harmonic oscillator description was used above 100 cm^{-1} while the free rotor description is used below this value and a damping function switches between the two expressions about this point, as previously described by Grimme.[33] Saddle points were connected to minima in the usual way with intrinsic reaction coordinate (IRC) calculations.[34] Computed structures are displayed with PyMol.[35]

The accurate computation of free energy changes for associative processes in solution remains a significant challenge, particularly since entropic terms associated with translation and rotation are hard to evaluate accurately in the condensed phase. A number of *post hoc* corrections have been employed in the literature, however, several have been criticized for their arbitrariness, and introducing unphysical assumptions.[36] We have treated the translational entropy according to the model developed by Shakhnovich, where the accessible free space associated with the solvent of interest is used instead of that which would be accessible to an ideal gas – this model reduces the magnitude of the S_{trans} relative to the gas phase, however, the dependence on temperature remains unchanged.[37] This was performed for acetic acid as solvent, to model pivalic acid, using a molarity for AcOH of 17.4 mol L^{-1} and a solvent volume (computed with B3LYP/6-31G*) of 86.1 $Å^3$ per molecule. This correction is justified in terms of the physical basis of this model, along with a correction to a 1 M standard state for all species except for benzene, which is present in a 40-fold excess, causing a corresponding increase in its chemical potential by RT ln(40). Nevertheless, we focus our analysis of computational results in terms of relative, rather than absolute predictions of reactivity. For example, the assessing the relative feasibility of initial possibilities for C–H activation relies on the comparison of **TS-1**, **TS-2**, **TS-3**, **TS-16** and **TS-17** which are structurally similar and identical in terms of the number of reacting species.

Acknowledgements

This research was supported financially by the Royal Society (RG110617), the European Community (FP7-PEOPLE-2012-IIF under grant agreement 330364 to QP), and Institute for Basic Science (IBS-R010-G1). We acknowledge the use of the EPSRC UK National Service for Computational Chemistry Software (CHEM773) in carry-ing out this work.

Notes and references

1 For selected reviews on *o*-C–H activation, see: (*a*) O. Daugulis, H.-Q. Do and D. Shabashov, *Acc. Chem. Res.*, 2009, **42**, 1074; (*b*) X. Chen, K. M. Engle, D.-H. Wang and J.-Q. Yu, *Angew. Chem., Int. Ed.*, 2009, **48**, 5094; (*c*) D. A. Colby, R. G. Bergman and J. A. Ellman, *Chem. Rev.*, 2010, **110**, 624; (*d*) T. W. Lyons and M. S. Sanford, *Chem. Rev.*, 2010, **110**, 1147; (*e*) S. H. Cho, J. Y. Kim, J. Kwak and S. Chang, *Chem. Soc. Rev.*, 2011, **40**, 5068; (*f*) C. Liu, H. Zhang, W. Shi and A. Lei, *Chem. Rev.*, 2011, **111**, 1780; (*g*) C.-L. Sun, B.-J. Li and Z.-J. Shi, *Chem. Rev.*, 2011, **111**, 1293; (*h*) C. S. Yeung and V. M. Dong, *Chem. Rev.*, 2011, **111**, 1215; (*i*) P. B. Arockiam, C. Bruneau and P. H. Dixneuf, *Chem. Rev.*, 2012, **112**, 5879; (*j*) N. Kuhl, M. N. Hopkinson, J. Wencel-Delord and F. Glorius, *Angew. Chem., Int. Ed.*, 2012, **51**, 10236; (*k*) S. R. Neufeldt and M. S. Sanford, *Acc. Chem. Res.*, 2012, **45**, 936; (*l*) M. S. Sigman and E. W. Werner, *Acc. Chem. Res.*, 2012, **45**, 874; (*m*) L. Ackermann, *Acc. Chem. Res.*, 2014, **47**, 281; (*n*) F. Zhang and D. R. Spring, *Chem. Soc. Rev.*, 2014, **43**, 6906; (*o*) J. J. Topczewski and M. S. Sanford, *Chem. Sci.*, 2015, **6**, 70.

2 (*a*) G. Brasche, J. García-Fortanet and S. L. Buchwald, *Org. Lett.*, 2008, **10**, 2207; (*b*) S. Rakshit, C. Grohmann, T. Besset and F. Glorius, *J. Am. Chem. Soc.*, 2011, **133**, 2350; (*c*) A. Deb, S. Bag, R. Kancherla and D. Maiti, *J. Am. Chem. Soc.*, 2014, **136**, 13602.

3 For examples of Pd catalyzed *m*-C–H activation by chelation assistance, see: (*a*) D. Leow, G. Li, T.-S. Mei and J.-Q. Yu, *Nature*, 2012, **486**, 518; (*b*) S. Lee, H. Lee and K. L. Tan, *J. Am. Chem. Soc.*, 2013, **135**, 18778; (*c*) H.-X. Dai, G. Li, X.-G. Zhang, A. F. Stepan and J.-Q. Yu, *J. Am. Chem. Soc.*, 2013, **135**, 7567; (*d*) R.-Y. Tang, G. Li and J.-Q. Yu, *Nature*, 2014, **507**, 215; (*e*) M. Bera, A. Modak, T. Patra, A. Maji and D. Maiti, *Org. Lett.*, 2014, **16**, 5760; (*f*) Y. Deng and J.-Q. Yu, *Angew. Chem., Int. Ed.*, 2015, **54**, 888; (*g*) M. Bera, A. Maji, S. K. Sahoo and D. Maiti, *Angew. Chem., Int. Ed.*, 2015, **54**, 8515; (*h*) S. Li, H. Ji, L. Cai and G. Li, *Chem. Sci.*, 2015, **6**, 5595.

4 For examples of *p*-C–H activation by chelation assistance: S. Bag, A. Maji, A. Hazra, M. Bera and D. Maiti, *J. Am. Chem. Soc.*, 2015, **137**, 11888.

5 For selected reviews on computational studies of C–H activation: (*a*) P. E. M. Siegbahn and M. R. A. Blomberg, *Dalton Trans.*, 2009, 5832; (*b*) D. Balcells, E. Clot and O. Eisenstein, *Chem. Rev.*, 2010, **110**, 749; (*c*) S. I. Gorelsky, *Coord. Chem. Rev.*, 2013, **257**, 153; (*d*) Y. Boutadla, D. L. Davies, S. A. Macgregor and A. I. Poblador-Bahamonde, *Dalton Trans.*, 2009, 5820.

6 For reviews see: (*a*) G.-J. Cheng, X. Zhang, L. W. Chung, L. Xu and Y.-D. Wu, *J. Am. Chem. Soc.*, 2015, **137**, 1706; (*b*) T. Sperger, I. A. Sanhueza, I. Kalvet and F. Schoenebeck, *Chem. Rev.*, 2015, **115**, 9532 and references therein; specific examples: (*c*) I. A. Sanhueza, A. M. Wagner, M. S. Sanford and F. Schoenebeck, *Chem. Sci.*, 2013, **4**, 2767.

7 With pivalate: (*a*) M. Lafrance and K. Fagnou, *J. Am. Chem. Soc.*, 2006, **128**, 16496; with phosphate: (*b*) G. Jindal and R. B. Sunoj, *J. Am. Chem. Soc.*, 2014, **136**, 15998; (*c*) G. Jindal and R. B. Sunoj, *Org. Lett.*, 2015, **17**, 2874.

8 D. L. Davies, S. Donald and S. Macgregor, *J. Am. Chem. Soc.*, 2005, **127**, 13754.

9 (*a*) M. Lafrance and K. Fagnou, *J. Am. Chem. Soc.*, 2006, **128**, 16496; (*b*) M. Lafrance, C. N. Rowley, T. K. Woo and K. Fagnou, *J. Am. Chem. Soc.*, 2006, **128**, 8754; (*c*) D. García-Cuadrado, A. A. C. Braga, F. Maseras and A. M. Echavarren, *J. Am. Chem. Soc.*, 2006, **128**, 1066; (*d*) D. Garcia-Cuadrado, P. de Mendoza, A. A. C. Braga, F. Maseras and A. M. Echavarren, *J. Am. Chem. Soc.*, 2007, **129**, 6880; (*e*) S. I. Gorelsky, D. Laporte and K. Fagnou, *J. Am. Chem. Soc.*, 2008, **130**, 10848; (*f*) S. I. Gorelsky, D. Lapointe and K. Fagnou, *J. Org. Chem.*, 2012, **77**, 658; and for an overview of mechanistic work: (*g*) D. Lapointe and K. Fagnou, *Chem. Lett.*, 2010, **39**, 1118.

10 (*a*) D. G. Musaev, A. Kaledin, B.-F. Shi and J.-Q. Yu, *J. Am. Chem. Soc.*, 2012, **134**, 1690; (*b*) R. Giri, Y. Lan, P. Liu, K. N. Houk and J.-Q. Yu, *J. Am. Chem. Soc.*, 2012, **134**, 14118; (*c*) M. Travis, T. M. Figg, M. Wasa, J.-Q. Yu and D. G. Musaev, *J. Am. Chem. Soc.*, 2013, **135**, 14206; (*d*) A. P. Smalley and M. J. Gaunt, *J. Am. Chem. Soc.*, 2015, **137**, 10632.

11 (*a*) G.-J. Cheng, Y.-F. Yang, P. Liu, P. Chen, T.-Y. Sun, G. Li, X. Zhang, K. N. Houk, J.-Q. Yu and Y.-D. Wu, *J. Am. Chem. Soc.*, 2014, **136**, 894; (*b*) Y.-F. Yang, G.-J. Cheng, P. Liu, D. Leow, T.-Y. Sun, P. Chen, X. Zhang, J.-Q. Yu, Y.-D. Wu and K. N. Houk, *J. Am.Chem. Soc.*, 2014, **136**, 344.

12 (*a*) M. Catellani and G. P. Chiusoli, *J. Organomet. Chem.*, 1992, **425**, 151; (*b*) C. C. Hughes and D. Trauner, *Angew. Chem., Int. Ed.*, 2002, **41**, 1569; (*c*) E. J. Hennessy and S. L. Buchwald, *J. Am. Chem. Soc.*, 2003, **125**, 12084; (*d*) B. S. Lane, M. A. Brown and D. Sames, *J. Am. Chem. Soc.*, 2005, **127**, 8050.

13 (*a*) M. Min, H. Choe and S. Hong, *Asian J. Org. Chem.*, 2012, **1**, 47; (*b*) Y. Moon, D. Kwon and S. Hong, *Angew. Chem.*, 2012, **124**, 11495; (*c*) Experimentally, in the coupling of chromone with benzene we observe that $Pd(OPiv)_2$ gives 94:6 selectivity for C2-arylation ; (*d*) Y. Moon and S. Hong, *Chem. Commun.*, 2012, **48**, 7191.

14 B. Glover, K. A. Harvey, B. Lui, M. J. Sharp and M. F. Tymoschenko, *Org. Lett.*, 2003, **5**, 301.

15 (*a*) V. I. Sokolov, L. L. Troitskaya and O. A. Reutov, *J. Organomet. Chem.*, 1979, **182**, 537; (*b*) A. D. Ryabov, I. K. Sakodinskaya and A. K. Yatsimirsky, *J. Chem. Soc., Dalton Trans.*, 1985, 2629; (*c*) M. Gomez, J. Granell and M. Martinez, *Organometallics*, 1997, **16**, 2539; (*d*) M. Gomez, J. Granell and M. Martinez, *J. Chem. Soc., Dalton Trans.*, 1998, 37; (*e*) B. Biswas, M. Sugimoto and S. Sakaki, *Organometallics*, 2000, **19**, 3895.

16 A. Petit, J. Flygare, A. T. Miller, G. Winkel and D. H. Ess, *Org. Lett.*, 2012, **14**, 3680.

17 (*a*) J. C. Holder, L. Zou, A. N. Marziale, P. Liu, Y. Lan, M. Gatti, K. Kikushima, K. N. Houk and B. M. Stoltz, *J. Am. Chem. Soc.*, 2013, **135**, 14996; (*b*) S. E. Walker, J. A. Jordan-Hore, D. G. Johnson, S. A. Macgregor and A.-L. Lee, *Angew. Chem., Int. Ed.*, 2014, **53**, 13876; (*c*) C. L. Boeser, J. C. Holder, B. L. H. Taylor, K. N. Houk, B. M. Stoltz and R. N. Zare, *Chem. Sci.*, 2015, **6**, 1917.

18 S. E. Walker, J. Boehnke, P. E. Glen, S. Levey, L. Patrick, J. A. Jor-dan-Hore and A.-L. Lee, *Org. Lett.*, 2013, **15**, 1886.

19 (*a*) D. Kim and S. Hong, *Org. Lett.*, 2011, **13**, 4466; (*b*) M. Min, Y. Kim and S. Hong, *Chem. Commun.*, 2013, **49**, 196; (*c*) M. Min and S. Hong, *Chem. Commun.*, 2012, **48**, 9613.

20 E. M. Simmons and J. F. Hartwig, *Angew. Chem., Int. Ed.*, 2012, **51**, 3066.

21 D. Wang, Y. Izawa and S. S. Stahl, *J. Am. Chem. Soc.*, 2014, **136**, 9914.

22 (*a*) T. A. Dwight, N. R. Rue, D. Charyk, R. Josselyn and B. DeBoef, *Org. Lett.*, 2007, **9**, 3137; (*b*) N. A. B. Juwaini, J. K. P. Ng and J. Seayad, *ACS Catal.*, 2012, **2**, 1787; (*c*) S. Potavathri, K. C. Pereira, S. I. Gorelsky, A. Pike, A. P. LeBris and B. DeBoef, *J. Am. Chem. Soc.*, 2010, **132**, 14676; (*d*) H. Li, J. Liu, C.-L. Sun, B.-J. Li and Z.-J. Shi, *Org. Lett.*, 2011, **13**, 276; (*e*) A. N. Campbell, E. B. Meyer and S. S. Stahl, *Chem. Commun.*, 2011, **47**, 10257; (*f*) C.-Y. He, Q.-Q. Min and X. Zhang, *Organometallics*, 2012, **31**, 1335; (*g*) Z. Li, L. Ma, J. Xu, L. Kong, X. Wu and H. Yao, *Chem. Commun.*, 2012, **48**, 3763; (*h*) G. Wu, J. Zhou, M. Zhang, P. Hu and W. Su, *Chem. Commun.*, 2012, **48**, 8964; (*i*) F. Chen, Z. Feng, C.-Y. He, H.-Y. Wang, Y.-L. Guo and X. Zhang, *Org. Lett.*, 2012, **14**, 1176; (*j*) B. Liu, Y. Huang, J. Lan, F. Song and J. You, *Chem. Sci.*, 2013, **4**, 2163; (*k*) X. Chen, X. Huang, Q. He, Y. Xie and C. Yang, *Chem. Commun.*, 2014, **50**, 3996.

23 (*a*) H. Ge, M. J. Niphakis and G. I. Georg, *J. Am. Chem. Soc.*, 2008, **130**, 3708; (*b*) Y. W. Kim, M. J. Niphakis and G. I. Georg, *J. Org. Chem.*, 2012, **77**, 9496; (*c*) Y.-Y. Yu, L. Bi and G. I. Georg, *J. Org. Chem.*, 2013, **78**, 6163.
24 S. Kozuch and S. Shaik, *Acc. Chem. Res.*, 2009, **42**, 1074.
25 M. Brookhart, M. L. H. Green and G. Parkin, *Proc. Natl. Acad. Sci. U. S. A.*, 2007, **104**, 6908.
26 M. J. Frisch, *et al.*, *Gaussian 09, Revision D.01*, Gaussian, Inc., Wallingford CT, 2009.
27 J.-D. Chai and M. Head-Gordon, *Phys. Chem. Chem. Phys.*, 2008, **10**, 6615.
28 W. R. Wadt and P. J. Hay, *J. Chem. Phys.*, 1985, **82**, 284.
29 L. E. Roy, P. J. Hay and R. L. Martin, *J. Chem. Theory Comput.*, 2008, **4**, 1029.
30 (*a*) A. D. Becke, *J. Chem. Phys.*, 1993, **98**, 5648; (*b*) C. Lee, W. Yang and R. G. Parr, *Phys. Rev. B*, 1988, **37**, 785; (*c*) S. H. Vosko, L. Wilk and M. Nusair, *Can. J. Phys.*, 1980, **58**, 1200; (*d*) P. J. Stephens, F. J. Devlin, C. F. Chabalowski and M. J. Frisch, *J. Phys. Chem.*, 1994, **98**, 11623.
31 S. Grimme, J. Antony, S. Ehrlich and H. Krieg, *J. Chem. Phys.*, 2010, **132**, 154104.
32 M. Cossi, N. Rega, G. Scalmani and V. Barone, *J. Comput. Chem.*, 2003, **24**, 669.
33 (*a*) S. Grimme, S. Ehrlich and L. Georigk, *J. Comput. Chem.*, 2011, **32**, 1456; (*b*) S. Grimme, *Chem.–Eur. J.*, 2012, **18**, 9955.
34 (*a*) H. P. Hratchian and H. B. Schlegel, *J. Chem. Phys.*, 2004, **120**, 9918; (*b*) H. P. Hratchian and H. B. Schlegel, *J. Chem. Theory Comput.*, 2005, **1**, 61.
35 *The PyMOL Molecular Graphics System, Version 1.5.0.4*, Schrödinger, LLC.
36 R. E. Plata and D. A. Singleton, *J. Am. Chem. Soc.*, 2015, **137**, 3811.
37 M. Mammen, E. I. Shakhnovich, J. M. Deutch and G. M. Whitesides, *J. Org. Chem.*, 1998, **63**, 3821.
38 Calculations for a model N–H enaminone substrate show a similarly high preference for C–H activation at the C3-position over C2 (NMe $\Delta\Delta G$ = 13.5 kcal mol^{-1}; N–H $\Delta\Delta G$ = 14.6 kcal mol^{-1}) indicating that steric interactions due to the *N*-methyl group are not decisive.